Nickel(II) Complexes Bearing the Bis(β-ketoamino) Ligand for the Copolymerization of Norbornene with a Higher 1-Alkene

Yuepeng Xing,[1,2] Yiwang Chen,[1] Xiaohui He,[1] Huarong Nie[1]

[1]*Institute of Polymers, Nanchang University, 999 Xuefu Avenue, Nanchang 330031, China*
[2]*School of Material Science and Engineering, Nanchang Hangkong University, 696 Fenghe South Avenue, Nanchang 330063, China*

Received 1 November 2010; accepted 29 December 2010
DOI 10.1002/app.34110
Published online 18 October 2011 in Wiley Online Library (wileyonlinelibrary.com).

ABSTRACT: A novel bis(β-ketoamino)Ni(II) complex catalyst, Ni{$CF_3C(O)CHC[N(naphthyl)]CH_3$}$_2$, was synthesized, and the structure was solved by a single-crystal X-ray refraction technique. The copolymerization of norbornene with higher 1-alkene was carried out in toluene with catalytic systems based on nickel(II) complexes, Ni{$RC(O)CHC[N(naphthyl)]CH_3$}$_2$(R=$CH_3$, CF_3) and $B(C_6F_5)_3$, and high activity was exhibited by both catalytic systems. The effects of the catalyst structure and comonomer feed content on the polymerization activity and the incorporation rates were investigated. The reactivity ratios were determined to be $r_{1\text{-octene}} = 0.009$ and $r_{\text{norbornene}} = 13.461$ by the Kelen–Tüdõs method for the Ni{$CH_3C(O)CHC[N(naphthyl)]CH_3$}$_2$/$B(C_6F_5)_3$ system. The achieved copolymers were confirmed to be vinyl-addition copolymers through the analysis of ^{1}H-NMR and ^{13}C-NMR. The thermogravimetric analysis results showed that the copolymers exhibited good thermal stability (decomposition temperature, $T_{dec} > 400$°C), and the glass-transition temperature of the copolymers were observed between 215 and 275°C. The copolymers were confirmed to be noncrystalline by wide-angle X-ray diffraction analysis and showed good solubility in common organic solvents. © 2011 Wiley Periodicals, Inc. J Appl Polym Sci 124: 1323–1332, 2012

Key words: addition polymerization; copolymerization; metal–organic catalysts/organometallic

INTRODUCTION

Interest in polymers of cyclic olefins, such as norbornene (NB; bicyclo-[2.2.1]hept-2-ene), has increased dramatically over the past decade because of their high chemical resistance, good UV resistance, high glass-transition temperature (T_g), low dielectric constant, excellent transparency, large refractive index, and low birefringence.[1–7] The vinyl polynorbornenes (PNBs), however, also exhibit some negative properties. For example, they are normally brittle at room temperature and have poor solubility in common organic solvents. In addition, the materials exhibit poor processability because of their high T_g values.[8] To improve their properties, a series of copolymers of NB with ethylene,[9,10] propylene,[11,12] NB derivatives,[13–15] and polar-group-terminal olefin monomer,[16] have also been studied.

On the other hand, only a few articles have reported the copolymerization of NB and a higher 1-alkene. The LG Chemical Group conducted the copolymerization of propylene, 1-hexene, and 1-octene using $H_2C(Me_2C_5H_2)_2ZrCl_2$–methylaluminoxane.[17] Kaminsky et al.[18] conducted the copolymerization of NB and 1-hexene using several metallocene catalysts. Hou et al.[19] reported the copolymerization of 1-hexene and dicyclopentadiene with a cationic CpSc complex. Shiono et al.[20] reported the copolymerization of NB and a higher 1-alkene with $Me_2Si(\eta^1\text{-}N^tBu)$(fluorenyl)$TiMe_2$ as a catalyst activated by $Ph_3CB(C_6F_5)_4$ in the presence of trioctyaluminum. However, the copolymerization of NB and a higher 1-alkene conducted by a catalyst based on a late-transition-metal complex has not been reported yet. So, we were interested in synthesizing novel late-transition-metal catalysts and copolymerizing NB with a 1-alkene to study the relationship between the catalyst structure and activity and the effect of different 1-alkene structure on the copolymer properties.

As we know, a little variation of the ligand structure may lead to a profound change in the catalytic reactivity. In this article, we report the synthesis of

Additional Supporting Information may be found in the online version of this article.

Correspondence to: Y. Chen (ywchen@ncu.edu.cn) or X. He (hexiaohuishulei@yahoo.com.cn).

Contract grant sponsor: Program for International Cooperation (Jiangxi Provincial Department of Science and Technology); contract grant number: 2009BHC00200.

Contract grant sponsor: Program for Innovative Research Team in University of Jiangxi Province.

two nickel(II) complexes with β-ketoamino chelate ligands and their copolymerization behavior toward NB and a higher 1-alkene after activation with $B(C_6F_5)_3$. The structure of the novel catalyst, Ni{CF_3-C(O)CHC[N(naphthyl)]CH_3}$_2$, was determined with a single-crystal X-ray refraction technique (see the Supporting Information for the crystallographic information file (CIF) data). The effects of the catalyst structure and comonomer feed content on the polymerization activity and incorporation rates were also investigated in detail. The reactivity ratios were determined by the Kelen–Tüdõs method.

EXPERIMENTAL

Materials

All manipulations involving air- and moisture-sensitive compounds were performed in a dried and purified argon atmosphere standard glovebox and with the Schlenk techniques. Toluene was dried over sodium/benzophenone and distilled under argon. NB was purified by distillation over sodium and used as a solution (4.25 mol/L) in toluene. The higher 1-alkene was purchased from Acros Organics (Shanghai, China) and was purified by two washings with aqueous sodium hydroxide(5.0 wt %) and two washings with water to remove the inhibitors; this was followed by drying over anhydrous $CaCl_2$ and distillation over CaH_2 under an argon atmosphere at reduced pressure. Other commercially available reagents were purchased and used without purification.

Preparation of the bis(β-ketoamino)Ni(II) complexes

The bis(β-ketoamino)Ni(II) complexes, Ni{R-C(O)CHC[N(naphthyl)]CH_3}$_2$(R=CH_3, CF_3), were synthesized according to a method reported in our previous work,[21] and the structure of Ni{CH_3-C(O)CHC[N(naphthyl)]CH_3}$_2$ was characterized in the literature.[21]

{CF_3C(O)CHC[HN(naphthyl)]CH_3}

1,1,1-Trifluoro-2,4-pentanedione (5 mL, 0.041 mol), 1-naphthylamine(5.871 g, 0.041 mol), and a catalytic amount of *p*-toluene sulfonic acid in toluene (150 mL) were combined and refluxed for 2–3 h. Water was removed as a toluene azeotrope at 125–130°C with a water separator. Volatiles were removed *in vacuo*, and recrystallization from hexane gave {CF_3C(O)CHC[HN(naphthyl)]CH_3} (6.2 g, 54%):

mp = 73°C. ^{1}H-NMR ($CDCl_3$, δ, ppm): 12.83 (s, 1H, O—H), 7.33–7.94 (m, 7H, naphthyl—H), 5.68 (s, 1H, C—$H_{backbone}$), 2.01(s, 3H, —CH_3).

Ni{CF_3C(O)CHC[N(naphthyl)]CH_3}$_2$

Potassium (0.4 g, 0.01 mol) was added to 25 mL of dried ^{t}BuOH. After the potassium dissolved, the solution was heated to 50°C, and {CF_3C(O)CHC[HN(naphthyl)]CH_3} (1.40 g, 0.005 mol) was added. The solution changed to yellow–orange as {CF_3C(O)CHC[HN(naphthyl)]CH_3} completely reacted with ^{t}BuOK. The reaction mixture was stirred for another 20 min. The solution was then slowly cooled to room temperature, and $[Et_4N]_2[NiBr_4]$ (1.586 g, 0.0025 mol) was introduced; the reacting mixture immediately formed a dark green precipitate. After vigorous stirring for several hours at room temperature, the excess ^{t}BuOH was removed *in vacuo*. The reaction slurry was extracted successively with hot toluene, and the mixture was filtered quickly. The filtrate was allowed to crystallize by slow cooling overnight. The product was isolated and dried under reduced pressure. Additional recrystallization from the *n*-hexane/toluene mixture solution gave blocks of red crystals.

Yield = 0.511 g, 33%. ^{1}H-NMR ($CDCl_3$, δ, ppm): 7.21–8.00 (m, 14H, naphthyl—H), 6.21 (s, 2H, C—$H_{backbone}$), 0.75–1.40 (m, 6H, —CH_3).

Structure solution and refinement for the complex Ni{CF_3C(O)CHC[N(naphthyl)]CH_3}$_2$

For the complex Ni{CF_3C(O)CHC[N(naphthyl)]CH_3}$_2$, a single crystal suitable for X-ray analysis was sealed in a glass capillary, and the intensity data of the single crystal were collected on a charge coupled device (CCD) Bruker Smart APEX II system. All determinations of the unit cell and intensity data were performed with graphite–monochromated Mo Kα radiation (λ = 0.71073 Å). All data were collected at room temperature with the ω scan technique is a way to obtain more detailed crystal data by XRD measurement and it is also called ω/2θ scan technique or Ω/2θ-scan technique. The structure was solved by a direct method with Fourier techniques and refined on F^2 by a full-matrix least-squares method. All of the nonhydrogen atoms were refined anisotropically, and all of the hydrogen atoms were included but not refined.

Polymerization

All of the procedures were carried out under a purified nitrogen atmosphere. A typical copolymerization procedure was as follows: a toluene solution of NB and the higher 1-alkene was added via a syringe to a 100-mL, two-necked, round-bottom flask containing a magnetic stirrer. The Ni(II) complex solution was then introduced followed by the $B(C_6F_5)_3$ solution. The total volume was kept constant at 10 mL. The polymerization reaction was performed for an appropriate time at a controlled temperature.

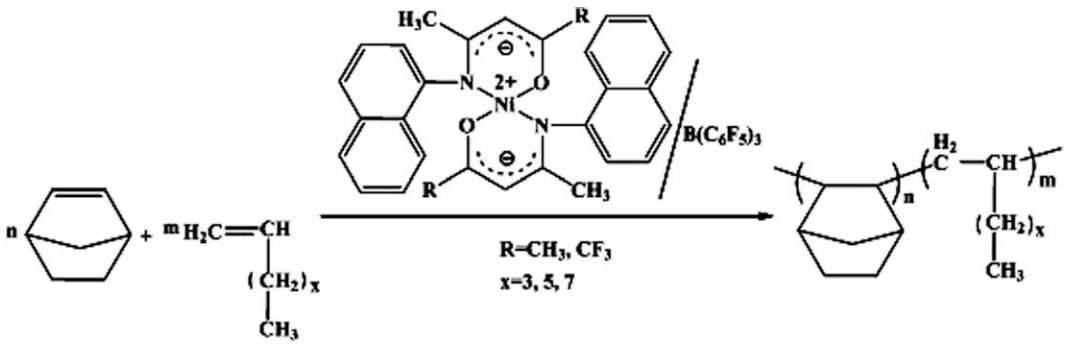

Scheme 1 Copolymerization of NB and 1-alkene catalyzed by the bis(β-ketoamino)Ni(II)/$B(C_6F_5)_3$ catalytic systems.

TABLE I
Crystal Data and Summary of Data Collection and Refinement Details for Complex Ni{$CF_3C(O)CHC[N(naphthyl)]CH_3$}$_2$

Empirical formula	$C_{30}H_{22}F_6N_2NiO_2$
Formula weight	615.21
Color	Red
Crystal system	Monoclinic
Space group	P2(1)/C
a (Å)	12.163 (5)
b (Å)	17.761 (7)
c (Å)	6.192 (3)
α (°)	90
β (°)	99.381 (4)
γ (°)	90
V (Å^3)	1319.7 (9)
Z	2
D_c (mg/m^3)	1.548
Absorption coefficient (Abs. coeff). (mm^{-1})	0.810
F(000)	628
Crystal size (mm)	0.384 × 0.195 × 0.124
θ limit (°)	2.85/28.31
Index ranges	$-16 \le h \le 16$
	$-20 \le k \le 23$
	$-8 \le l \le 8$
Number of observed reflections	3242
Number of parameters refined	187
Goodness of fit on F^2	1.061
Final *R* indices [$I > 2\sigma(I)$]	0.0820, 0.2388
R indices (all data)	0.1199, 0.2642

$R = \Sigma| \ |F_o| - |F_c| \ |\Sigma \ |F_o|$; $R_w = [\Sigma_w(F_o^2 - F_c^2)^2 / \Sigma_w(F_o^2)^2]^{1/2}$.

The size and shape of the unit cell can be described by three lattice vectors: *a*, *b*, *c* or the axial lengths *a*, *b*, and *c* and inter axial angels α, β, and γ; *V* is the unit cell volume in Å^3; *Z* is the number of molecules in a unit cell; D_c is the crystal density in mg/m^3; *F*(000) is the numbers of electrons in each unit cell; θ limits is the range of diffraction angle in degrees. Goodness-of-fit on F^2 means a method to refine a crystal data. Shelxl always refines against F^2 and when the data of goodness-of-fit on F^2 are approaching to 1 that means the crystal solution is correct. Final R indices [$I > 2\sigma$(I)] means the final residual *R* value and the data should be very small. R indices (all data) means the all residual *R* value and the data should be very small. *h*, *k*, and *l* are the crystal plane indices corresponding to diffraction peaks.

The numbers in parentheses indicate standard deviation. For example the number 1.822(4) is equal to 1.822±0.004.

The reaction was terminated by the addition of acidic ethanol (90:10 ethanol/HCl). The resulting precipitated polymers were collected by filtration and washed with ethanol several times and dried *in vacuo* at 60°C. (The copolymerization procedure and the structure of the catalyst are shown in Scheme 1).

Characterization

The molecular weight and molecular weight distribution (MWD) of the polymers were measured by gel permeation chromatography (GPC) with a Waters Breeze Isocratic high performance liquid chromatograph (HPLC) instrument consisting of a Rheodyne injector, a 1515 Isocratic pump, a Waters 2414 differential refractometer, and a Styragel column set, Styragel HT3 and HT4, to separate molecular weights ranging from 10^2 to 10^6. The oven temperature was set at 40°C. Chloroform was used as the eluent, and the flow rate was 1 mL/min. Monodispersed polystyrene standards (Aldrich Chemical, Shanghai, China) were used to generate the calibration curve. ^{1}H-NMR and ^{13}C-NMR spectra of the polymers were carried out on a Bruker ARX 400 NMR spectrometer at room temperature with chloroform-*d* as the solvent and tetramethylsilane (δ = 0) as an internal reference. Thermogravimetric analysis (TGA) data were measured with a PerkinElmer TGA 7 thermogravimetric (Waltham, USA) analyzer thermal analysis system under a nitrogen atmosphere up to 650°C at a heating rate of 10°C/min. The T_g values of the copolymers were determined by differential scanning calorimetry (DSC) with a Shimadzu DSC-60 instrument (Tokyo, Japan) at a heating rate of 10°C/min. The wide-angle X-ray diffraction (WAXD) curves of the polymer powders were obtained with a Bruker D8 Focus X-ray diffractometer with monochromatic radiation at a wavelength of 1.54 Å at a scanning rate of 2°/min. Scanning was performed with 2θ ranging from 2 to 70°.

TABLE II
Selected Bond Lengths and Angles for the Complex Ni{$CF_3C(O)CHC[N(naphthyl)]CH_3$}$_2$

Bond	Length (Å)	Bond	Angle (°)
Ni(1)—O(1)#1	1.822 (4)	O(1)#1—Ni(1)—O(1)	180.0 (4)
Ni(1)—O(1)	1.822 (4)	O(1)#1—Ni(1)—N(1)#1	92.64 (18)
Ni(1)—N(1)#1	1.932 (4)	O(1)—Ni(1)—N(1)#1	87.36 (18)
Ni(1)—N(1)	1.932 (4)	O(1)#1—Ni(1)—N(1)	87.36 (17)
O(1)—C(13)	1.273 (7)	O(1)—Ni(1)—N(1)	92.64 (18)
N(1)—C(11)	1.305 (7)	N(1)#1—Ni(1)—N(1)	180.0
N(1)—C(9)	1.450 (6)	C(13)—O(1)—Ni(1)	125.9 (4)
C(9)—C(10)	1.355 (8)	C(11)—N(1)—C(9)	116.5 (4)
C(9)—C(8)	1.418 (7)	C(11)—N(1)—Ni(1)	125.5 (4)
C(12)—C(13)	1.350 (8)	C(9)—N(1)—Ni(1)	118.0 (3)
C(12)—C(11)	1.428 (8)	C(10)—C(9)—C(8)	121.1 (5)
C(8)—C(3)	1.419 (8)	C(10)—C(9)—N(1)	121.0 (5)
C(8)—C(7)	1.419 (8)	C(8)—C(9)—N(1)	117.9 (5)
C(13)—C(15)	1.520 (8)	C(13)—C(12)—C(11)	121.9 (5)
F(1)—C(15)	1.309 (8)	C(9)—C(8)—C(3)	117.9 (5)
C(3)—C(2)	1.413 (9)	C(9)—C(8)—C(7)	122.4 (5)
C(3)—C(4)	1.424 (9)	C(3)—C(8)—C(7)	119.7 (5)
C(11)—C(14)	1.510 (8)	O(1)—C(13)—C(12)	128.2 (5)
F(3)—C(15)	1.295 (8)	O(1)—C(13)—C(15)	112.5 (5)
C(10)—C(1)	1.405 (8)	C(12)—C(13)—C(15)	119.2 (5)
C(7)—C(6)	1.376 (8)	C(2)—C(3)—C(8)	119.7 (5)
F(2)—C(15)	1.347 (9)	C(2)—C(3)—C(4)	122.4 (6)
C(4)—C(5)	1.366 (11)	C(8)—C(3)—C(4)	117.9 (6)
C(1)—C(2)	1.347 (10)	N(1)—C(11)—C(12)	122.3 (5)
C(5)—C(6)	1.387 (11)	N(1)—C(11)—C(14)	121.6 (5)
		C(12)—C(11)—C(14)	116.1 (5)
		C(9)—C(10)—C(1)	120.2 (6)
		C(6)—C(7)—C(8)	119.8 (6)
		C(5)—C(4)—C(3)	121.0 (6)
		C(2)—C(1)—C(10)	121.0 (6)
		C(1)—C(2)—C(3)	120.2 (6)
		F(3)—C(15)—F(1)	108.8 (6)
		F(3)—C(15)—F(2)	105.4 (6)
		F(1)—C(15)—F(2)	105.6 (6)
		F(3)—C(15)—C(13)	114.8 (6)
		F(1)—C(15)—C(13)	111.4 (5)
		F(2)—C(15)—C(13)	110.3 (6)
		C(4)—C(5)—C(6)	120.6 (6)
		C(7)—C(6)—C(5)	120.9 (7)

RESULTS AND DISCUSSION

Structure analyses

A single crystal of the complex Ni{$CF_3C(O)CHC[N(naphthyl)]CH_3$}$_2$ suitable for X-ray diffraction was grown from a concentrated toluene solution at room temperature. The crystallographic data are summarized in Table I. Table II lists the selected bond lengths and angles. The Oak Ridge Thermal Ellipsoid Plot (ORTEP) diagram of the complex is shown in Figure 1.

As depicted in Figure 1, the crystal structures of the complex Ni{$CF_3C(O)CHC[N(naphthyl)]CH_3$}$_2$ were similar to those of the analogue complexes we previously reported,[21,22] and all shared the four-coordination binding mode around a nickel(II) center.

Copolymerization of NB and the higher 1-alkene

In this work, two different bis(β-ketoamino)Ni(II) complexes, containing various steric and electronic ligands, were used to investigate the influence of the catalyst framework on the polymerization activity and incorporation rates. The results of the copolymerization of NB and the higher 1-alkene with various bis(β-ketoamino)Ni(II)/$B(C_6F_5)_3$ catalytic systems and comonomer feed contents are summarized in Tables III and IV.

The 1-alkene contents thus obtained are shown in Tables III and IV, which indicates that the 1-alkene content could be controlled with the feedstock composition of 1-alkene. Moreover, the weight-average molecular weights (M_w's) and T_g of the copolymers were dependent on the 1-decene feed content. On the other hand, the yield and activity depended on the kind of 1-alkene and increased in the order of 1-Hexene > 1-Octene > 1-Decene, as the literature reported.[20] The use of catalysts with differently substituted ligands had an effect on the polymerization activity because of the various steric and electronic interactions between the ligand and 1-alkene. The activities detected in the copolymerization of NB and 1-alkene with the Ni{$CH_3C(O)CHC[N(naphthyl)]CH_3$}$_2$/$B(C_6F_5)_3$ system were somewhat lower in comparison with the activities observed with Ni{$CF_3C(O)CHC[N(naphthyl)]CH_3$}$_2$/$B(C_6F_5)_3$. Similar results were reported in the literature[23] and indicate that the CF_3 group with a strong electron-withdrawing effect is beneficial to the catalytic activity toward the copolymerization.

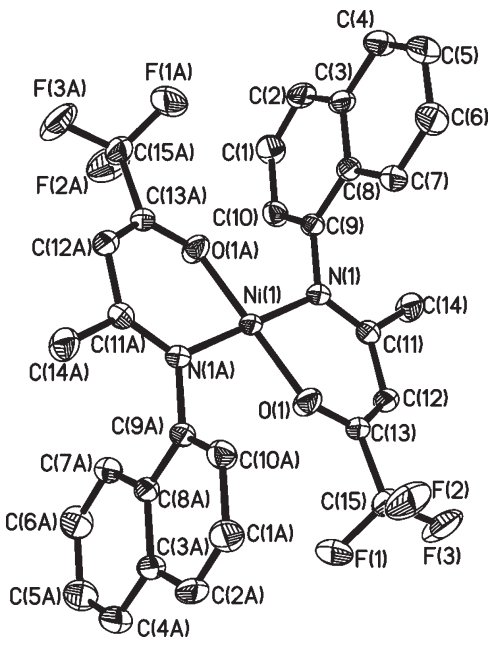

Figure 1 ORTEP plots of the Ni{$CF_3C(O)CHC[N(naphthyl)]CH_3$}$_2$ complex. The atom labeling scheme is shown; hydrogen atoms were omitted for clarity.

TABLE III
Copolymerization of NB and 1-Alkene Catalyzed by the Ni{$CH_3C(O)CHC[N(naphthyl)]CH_3$}$_2$/B($C_6F_5$)$_3$ System

Entry	Comonomer	NB/1-alkene	Yield (%)[a]	Activity [g of polymer (mol of Ni)$^{-1}$·h^{-1}]	$M_w \times 10^{-4}$ (g/mol)	MWD	1-alkene (mol %)[b]	T_g (°C)
1	—	100/0	100	3.20×10^4	—[c]	—[c]	0	—[c]
2	1-Hexene	90/10	52.0	1.62×10^4	5.8	1.69	8.64	273.5
3	1-Hexene	70/30	31.6	0.97×10^4	3.0	1.89	10.36	260.2
4	1-Hexene	50/50	13.6	0.41×10^4	1.5	2.17	12.85	252.6
5	1-Hexene	0/100	Trace	—[c]	—[c]	—[c]	—[c]	—[c]
6	1-Octene	90/10	47.4	1.52×10^4	5.9	1.64	8.61	272.9
7	1-Octene	70/30	28.4	0.94×10^4	3.6	1.77	9.16	265.3
8	1-Octene	50/50	15.4	0.53×10^4	2.7	2.01	11.83	243.2
9	1-Octene	0/100	Trace	—[c]	—[c]	—[c]	—[c]	—[c]
10	1-Decene	90/10	41.1	1.36×10^4	8.7	1.45	8.22	263.5
11	1-Decene	70/30	30.0	1.08×10^4	5.1	1.73	10.21	235.9
12	1-Decene	50/50	13.8	0.54×10^4	2.0	2.50	10.54	216.8
13	1-Decene	0/100	Trace	—[c]	—[c]	—[c]	—[c]	—[c]

[a] Conditions: catalyst concentration, c[Cat.] = 5.0×10^{-4} mol/L; n[NB] + n[1-alkene] = 0.01 mol, n[B]/n[Ni] = 20/1; n is the molar quantity of monomer, polymerization time, tp = 6 h, polymerization temperature, T_p = 60°C, solvent: toluene, polymerization volume, V_p = 10 mL.
[b] Determined from the ^{1}H-NMR spectra. Higher 1-alkene (mol %) = $I_{CH3}/(I_{CH3} + 1.5I_{C2/C3})$, where I_{CH3} represents the area of the methyl in the higher 1-alkene region and $I_{C2/C3}$ represents the area of the positions C_2 and C_3 methine in the NB (see Fig. 4).
[c] Not determined.

To determine the monomer reactivity ratios ($r_{1\text{-octene}}$ and $r_{\text{norbornene}}$), a series of experiments were performed and were catalyzed by the Ni{$CH_3C(O)CHC[N(naphthyl)]CH_3$}$_2$/B($C_6F_5$)$_3$ system with different initial comonomer feed concentrations and stopped at a low yield by control of the polymerization time. The results are shown in Table V. The reactivity ratios, determined by the Kelen–Tüdõs method[24] (Fig. 2), were $r_{1\text{-octene}}$ = 0.009 and $r_{\text{norbornene}}$ = 13.461, catalyzed by Ni{$CH_3C(O)CHC[N(naphthyl)]CH_3$}$_2$/B($C_6F_5$)$_3$ system; this illustrated that the reactivity of NB was higher than that of 1-octene.

As shown in Tables III and IV, the homopolymerization of the 1-alkene only produced trace polymer, and the copolymerization of NB with the 1-alkene produced copolymers with contents of the 1-alkene of about 7.85–14.29%. The phenomenon could be explained by the fact that both coordination and insertion of the NB monomer took place more easily than the corresponding reactions of α-olefin. The

TABLE IV
Copolymerization of NB and 1-Alkene Catalyzed by the Ni{$CF_3C(O)CHC[N(naphthyl)]CH_3$}$_2$/B($C_6F_5$)$_3$ System

Entry	Comonomer	NB/1-alkene	Yield (%)[a]	Activity [g of polymer (mol of Ni)$^{-1}$·h^{-1}]	$M_w \times 10^{-4}$ (g/mol)	MWD	1-alkene (mol %)[b]	T_g (°C)
14	—	100/0	100	3.20×10^4	—[c]	—[c]	0	—[c]
15	1-Hexene	90/10	58.3	1.82×10^4	9.9	1.44	7.85	275.9
16	1-Hexene	70/30	37.3	1.14×10^4	6.1	1.61	9.54	264.3
17	1-Hexene	50/50	22.3	0.67×10^4	3.0	1.84	14.29	240.1
18	1-Hexene	0/100	Trace	—[c]	—[c]	—[c]	—[c]	—[c]
19	1-Octene	90/10	55.3	1.77×10^4	8.9	1.48	8.46	274.3
20	1-Octene	70/30	33.7	1.12×10^4	7.8	1.65	10.74	260.3
21	1-Octene	50/50	16.2	0.56×10^4	3.1	1.77	13.56	240.7
22	1-Octene	0/100	Trace	—[c]	—[c]	—[c]	—[c]	—[c]
23	1-Decene	90/10	49.9	1.64×10^4	10.3	1.27	7.88	275.7
24	1-Decene	70/30	32.7	1.18×10^4	8.4	1.64	9.07	260.6
25	1-Decene	50/50	15.4	0.60×10^4	3.2	1.75	10.62	239.6
26	1-Decene	0/100	Trace	—[c]	—[c]	—[c]	—[c]	—[c]

[a] Conditions: c[Cat.] = 5.0×10^{-4} mol/L, n[NB] + n[1-alkene] = 0.01 mol, n[B]/n[Ni] = 20/1, tp = 6 h, T_p = 60°C, solvent: toluene, V_p = 10 mL.
[b] Determined from ^{1}H-NMR spectra. Higher 1-alkene (mol %) = $I_{CH3}/(I_{CH3} + 1.5I_{C2/C3})$, where I_{CH3} represents the area of the methyl in the higher 1-alkene region and $I_{C2/C3}$ represents the area of positions C_2 and C_3 methine in the NB (see Fig. 4).
[c] Not determined.

TABLE V
Copolymerization Results of NB and 1-Octene Catalyzed by the Ni{$CH_3C(O)CHC[N(naphthyl)]CH_3$}$_2$/$B(C_6F_5)_3$ System

1-Octene in the feed (mol %)	1-Octene incorporated (mol %)[a]	Yield (%)[c]	Polymerization time
10	—[b]	40.2	1 min
20	—[b]	21.3	2 min
30	—[b]	19.4	3 min
40	4.4	10.9	15 min
50	5.7	7.5	20 min
60	7.8	5.4	30 min
70	9.3	4.6	2 h
80	14.4	2.5	3 h

[a] Determined from ^{1}H-NMR spectra. Higher 1-alkene (mol %) = $I_{CH3}/(I_{CH3} + 1.5I_{C2/C3})$, where I_{CH3} represents the area of the methyl in the higher 1-alkene region and $I_{C2/C3}$ represents the area of the positions C_2 and C_3 methine in the NB (see Fig. 4).
[b] Not determined.
[c] Conditions: c[Cat.] = 5.0×10^{-4} mol/L, n[NB] + n[1-octene] = 0.01 mol, n[B]/n[Ni] = 20/1, T_p = 60°C, solvent: toluene, V_p = 10 mL.

yield and activity depended on the kind of 1-alkene and increased in the order of 1-Hexene > 1-Octene > 1-Decene; this may have been the effect of the steric hindrance of 1-alkene. The steric hindrance of poly(1-alkene) blocked the free coordination site at the Ni(II) active center conjecture, as shown in Scheme 2. The cocatalyst $B(C_6F_5)_3$ may have activated the catalyst and removed one of the ligands, as reported in the literature.[8] In the process of NB homopolymerization, NB could coordinate with the Ni(II) active center. After the first NB insertion, the propagation proceeded, and the polymer chains grew. Therefore, because the planar conformation, normally required for β-H elimination, of a Ni–PNB bond intermediate in the exo position and of the β-H–carbon bond in the endo position is prohibited by Bredt's rule,[25] the β-H elimination could not happen in the homopolymerization procedure of NB. In the process of 1-alkene homopolymerization after the coordination and insertion, the 1-alkene connected with the Ni(II) active center that formed, and then, the steric hindrance of 1-alkene side chains may have inhibited the continuous chain propagation. Therefore, only trace polymer was obtained in the homopolymerization of the 1-alkene. In the copolymerization of NB and the 1-alkene, NB coordinated with the Ni(II) active center because of its higher coordination and insertion ability. When 1-alkene was inserted into the polymer, the steric hindrance of the 1-alkene side chain inhibited the continuous chain propagation to a certain degree and may have led to a β-H elimination. When the 1-alkene content was increased in the feed, 1-alkene had more opportunities to insert into the polymer, the steric hindrance of the 1-alkene chain may have more effectively blocked the Ni(II) active center, and the probabilities of β-H elimination may have increased. Therefore, the yield and the activity decreased. Furthermore, with the 1-alkene's chain length increasing, the steric hindrance increased, and then, the yield and activity decreased.

GPC curve of the copolymer

The GPC curves of the NB/1-decene copolymers with different 1-decene molar ratios are shown in Figure 3, and the other GPC curves of the NB/1-alkene copolymers are familiar. The MWDs were close to 2.0 and appeared as a single modal in the GPC chromatogram; this indicated that copolymerizations occurred at the single active site and that the products were the true copolymers instead of blends of the homopolymers.[26] PNBs prepared by both the bis(β-ketoamino)Ni(II) and $B(C_6F_5)_3$ catalytic systems were soluble in cyclohexane. Moreover,

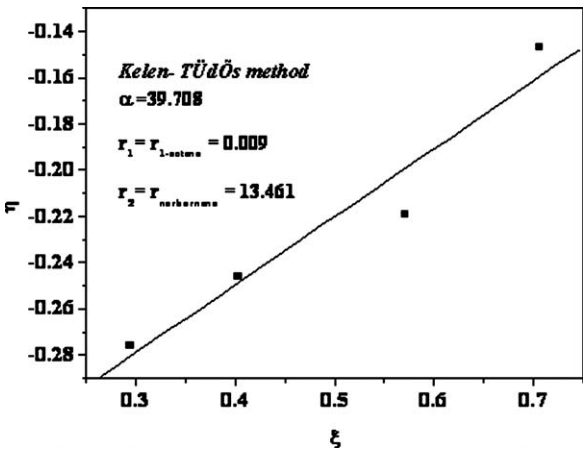

Figure 2 Linear fitting of the NB/1-octene copolymers catalyzed with the Ni{$CH_3C(O)CHC[N(naphthyl)]CH_3$}$_2$/$B(C_6F_5)_3$ system according to the Kelen–Tüdõs method: $\eta = \left(r_1 + \frac{r_2}{\alpha}\right)\xi - \frac{r_2}{\alpha}$, $\eta = \frac{G}{\alpha+F}$, $\xi = \frac{F}{\alpha+F}$, $G = \frac{x(y-1)}{y}$, $F = \frac{x^2}{y}$, $\alpha = \sqrt{F_{\min} \times F_{\max}}$, $x = \frac{[1-\text{Octene}]}{[\text{NB}]}$, $y = \frac{d[1-\text{Octene}]}{d[\text{NB}]}$. $x = \frac{[1-\text{Octene}]}{[\text{NB}]}$, and x means the molar ratio of 1-octene and NB in the beginning polymerization system. $y = \frac{d[1-\text{Octene}]}{d[\text{NB}]}$. and y means the molar ratio of 1-octene and NB in the polymers. r_1 and r_2 indicate the reactivity ratio of 1-octene and NB, respectively, and $r_1 = k_{11}/k_{12}$, $r_2 = k_{22}/k_{21}$. In the Kelen-TÜdÕs method, the parameters α, η, ξ, F, and G are used to calculate the r_1 and r_2 in the basis of x and y and the deviations may decrease comparing to Fineman Ross method. By the definition of the parameters α, η, ξ, F, and G, we can get a series of η, γ, then draw the plots according to each groups of η, ξ. Finally, by the linear fitting of these plots, we can get the equation $\eta = \left(r_1 + \frac{r_2}{\alpha}\right)\xi - \frac{r_2}{\alpha}$. So the slope is $(r_1 + r_2/\alpha)$ and the intercept is: r_2/α and then we can get r_1 and r_2.

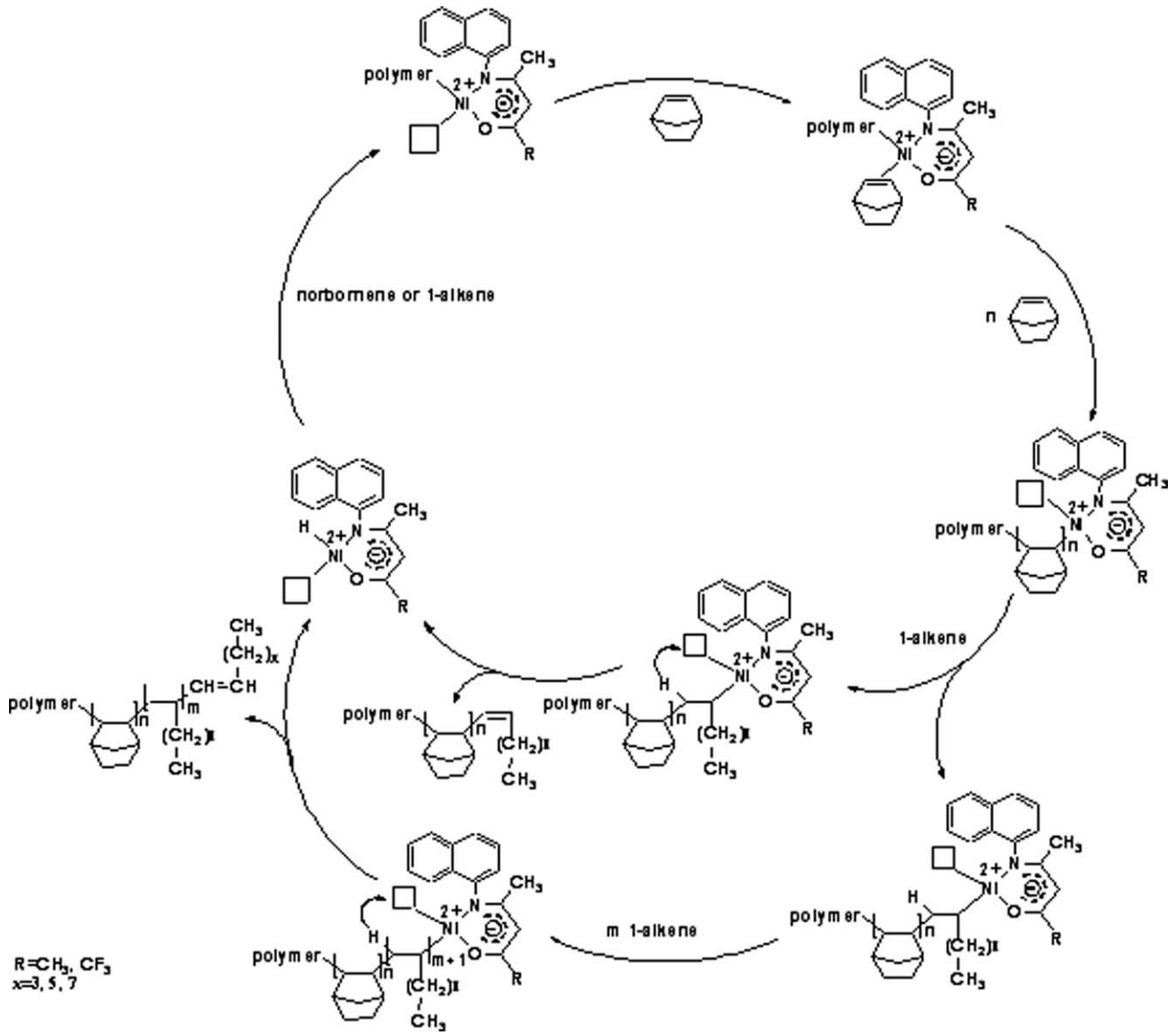

Scheme 2 Insertion mechanism, including the steric hindrance effect on the copolymerization of NB and 1-alkene catalyzed by the bis(β-ketoamino)Ni(II)/$B(C_6F_5)_3$ catalytic systems.

the copolymerization products were found to be dissolved completely in either cyclohexane or chloroform, whereas PNB was not dissolved in chloroform. These results give an impression of the high influence of the 1-alkene on the copolymerization product and proved that the products were true NB/1-alkene copolymers instead of blends of homopolymers.

^{1}H-NMR and ^{13}C-NMR spectra of the copolymers

Figure 4 shows the ^{1}H-NMR and ^{13}C-NMR spectra of the copolymers poly(nobornene-*co*-1-decene) obtained by the Ni{$CF_3C(O)CHC[N(naphthyl)]CH_3$}$_2$/$B(C_6F_5)_3$ system. As shown in Figure 4(A), four groups of resonance peaks appeared between 0.7 and 2.5 ppm in the ^{1}H-NMR spectrum of poly(nobornene-*co*-1-decene). The peak at 0.7–0.9 ppm could be attributed to the methyl hydrogen, corresponding to H^{10}, and the peak at 0.9–1.6 ppm could be attributed to methene hydrogens corresponding to $C^7/C^5/C^6/H^1/H^2/H^3/H^4/H^5/H^6/H^7/H^8/H^9$. The peak at 1.6–2.0 ppm could be attributed to the methine hydrogen corresponding to C^1/C^4, and the peak at 2.0–2.5 ppm could be attributed to the methine hydrogen corresponding to C^2/C^3. The weak peak at 5.3 ppm corresponded to internal vinylene groups and meant that the 1-alkene insertion followed a 2, 1 insertion pathway.[27] In addition, the absence of a significant resonance at 5.0–6.0 ppm indicated no large amounts of double bonds, which are typical for metathesis-type PNBs.[28]

As shown in Figure 4(B), four groups of resonance peaks appeared between 14 and 56 ppm in the ^{13}C-NMR spectrum of poly(norbornene-*co*-1-decene). The peak at 14 ppm could be attributed to the methyl carbon corresponding to H^{10}, that at 23 ppm could be

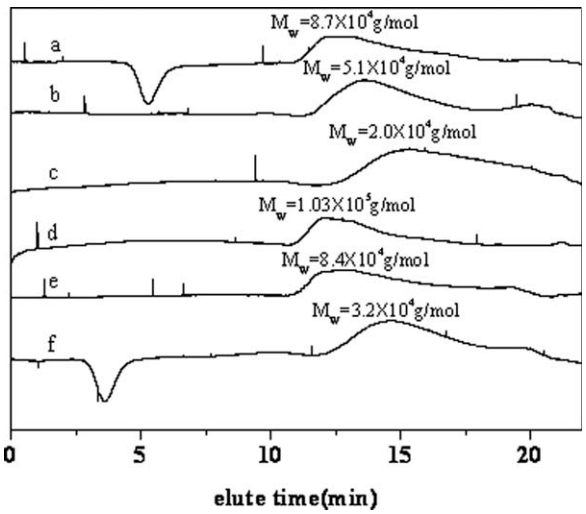

Figure 3 GPC curves of the NB/1-decene copolymers with different 1-decene molar ratios: (a) 8.21, (b) 10.22, and (c) 10.54% {with the Ni{$CH_3C(O)CHC[N(naphthyl)]CH_3\}_2$/$B(C_6F_5)_3$ system} and (d) 7.88, (e) 9.07, and (f) 10.62% {with the Ni{$CF_3C(O)CHC[N(naphthyl)]CH_3\}_2$/$B(C_6F_5)_3$ system}.

attributed to the methene carbon corresponding to H^9, that at 28–38 ppm could be attributed to the methene carbon corresponding to $C^7/C^5/C^6/H^1/H^2/H^3/H^4/H^5/H^6/H^7/H^8$, that at 38–44 ppm could be attributed to the methine carbon corresponding to C^1/C^4, and that at 44–56 ppm could be attributed to the methine carbon corresponding to C^2/C^3, respectively.

TGA and DSC analysis of the copolymer

TGA curves of poly(norbornene-*co*-1-alkene) with different 1-alkene contents prepared by the bis(β-ketoamino)Ni(II)/$B(C_6F_5)_3$ catalytic systems are shown in Figures 5–7. The thermal stabilities of all of the copolymers were similar, and decompositions occurred at high temperatures, from 370 to 450°C.

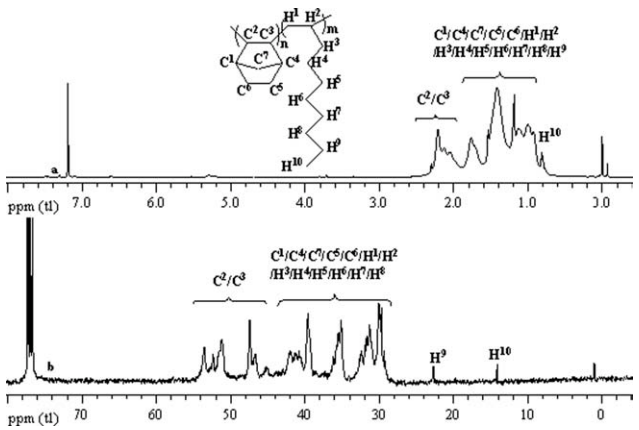

Figure 4 (a) ^{1}H-NMR and (b) ^{13}C-NMR spectra of poly(norbornene-*co*-1-decene) with a 9.07% molar ratio of 1-decene obtained by the Ni{$CF_3C(O)CHC[N(naphthyl)]CH_3\}_2$/$B(C_6F_5)_3$ system.

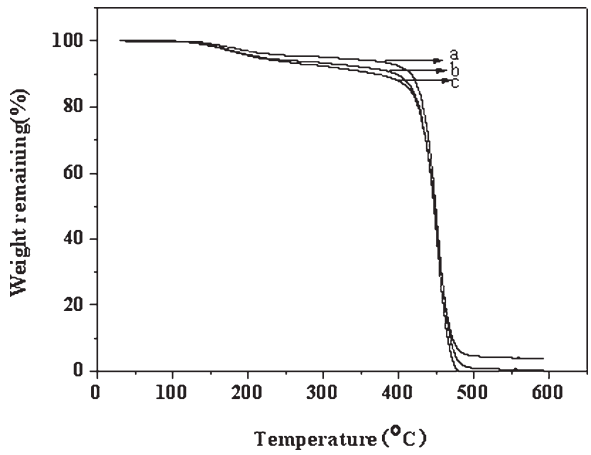

Figure 5 TGA thermograms of poly(norbornene-*co*-1-hexene) with (a) 8.64, (b) 10.36, and (c) 12.85% molar ratios of 1-hexene obtained by the Ni{$CH_3C(O)CHC[N(naphthyl)]CH_3\}_2$/$B(C_6F_5)_3$ system.

The decomposition temperature decreased with increasing 1-alkene content in the copolymers. The T_g values of the copolymers were investigated by DSC analyses, and the DSC curves of poly(norbornene-*co*-1-octene) are shown in Figure 8. The T_g values of the copolymers decreased as the 1-alkene molar ratio increased in the copolymers because 1-alkene had a relatively lower T_g. TGA and DSC analysis indicated that the copolymers obtained by the bis(β-ketoamino)Ni(II)/$B(C_6F_5)_3$ catalytic systems exhibited good thermostability under nitrogen.

WAXD of the copolymer

The powder WAXD patterns of poly(norbornene-1-alkene) with different 1-alkene contents prepared by the bis(β-ketoamino)Ni(II)/$B(C_6F_5)_3$ catalytic systems

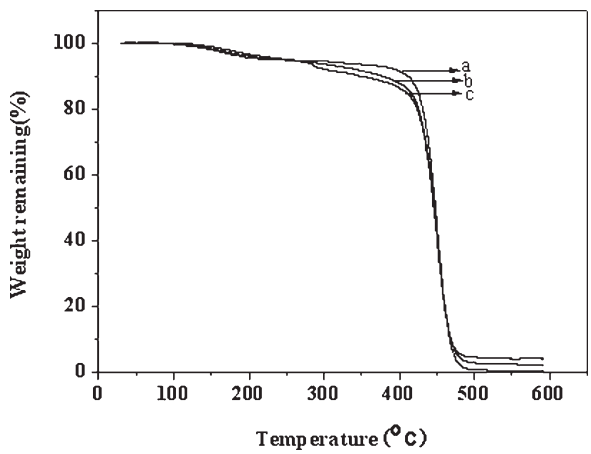

Figure 6 TGA thermograms of poly(norbornene-*co*-1-octene) with (a) 8.61, (b) 9.16, and (c) 11.83% molar ratios of 1-octene obtained by the Ni{$CH_3C(O)CHC[N(naphthyl)]CH_3\}_2$/$B(C_6F_5)_3$ system.

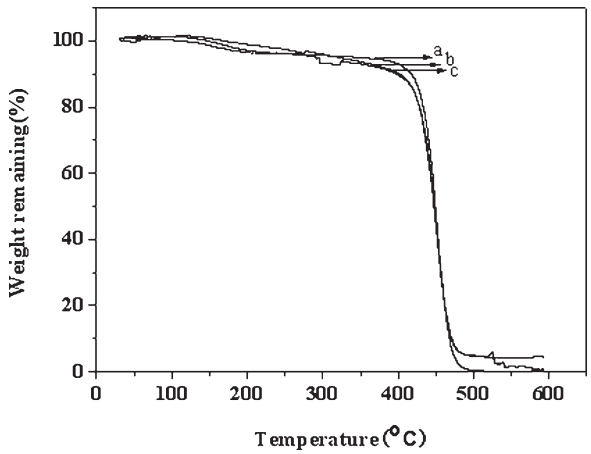

Figure 7 Figure 7 TGA thermograms of poly(norbornene-*co*-1-decene) with (a) 7.88, (b) 9.07, and (c) 10.62% molar ratios of 1-decene obtained by the Ni{$CF_3C(O)CHC[N(-naphthyl)]CH_3\}_2/B(C_6F_5)_3$ system.

are shown in Figure 9. Two broad halos at 2θ values of 10.43 and 18.64 were observed. The occurrence of two halos was characteristic for PNB, and the corresponding distances amounted to 8.50 and 4.77 Å.[29] No traces of Bragg reflections were revealed in the characteristic crystalline regions, and the polymers were, therefore, noncrystalline.[30]

CONCLUSIONS

A Ni{$CF_3C(O)CHC[N(naphthyl)]CH_3\}_2$ complex was synthesized, and the structure was solved by a single-crystal X-ray refraction technique. The copolymerizations of NB with a higher 1-alkene were catalyzed by Ni{$RC(O)CHC[N(naphthyl)]CH_3\}_2$ (R=CH_3, CF_3)/$B(C_6F_5)_3$ catalytic systems. This showed that an increase in the initial 1-alkene feed content led to an increase in the incorporated 1-alkene content of the resulting copolymer. The Ni{$CF_3C(O)CHC[N(naphthyl)]CH_3\}_2/B(C_6F_5)_3$ system was found to exhibit higher catalytic activity than the Ni{$CH_3C(O)CHC[N(naphthyl)]CH_3\}_2/B(C_6F_5)_3$ system. An insertion mechanism, including the steric hindrance effect on the copolymerization of NB and 1-alkene catalyzed by the bis(β-ketoamino)Ni(II)/$B(C_6F_5)_3$ catalytic systems, was proposed. The reactivity ratios were determined by the Kelen–Tüdõs method, and $r_{1\text{-octene}}$ was 0.009, and $r_{\text{norbornene}}$ was 13.461 for the Ni{$CH_3C(O)CHC[N(naphthyl)]CH_3\}_2/B(C_6F_5)_3$ system. The analyses of the copolymer structures and properties indicated that the copolymerization of NB and the higher 1-alkene occurred via a vinyl polymerization mode. The copolymers showed good thermostability (decomposition temperature, $T_{dec} > 400°C$) and were noncrystalline.

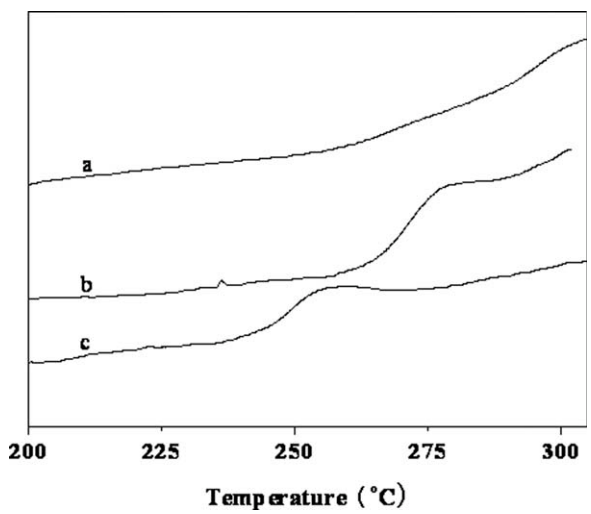

Figure 8 DSC curves of poly(norbornene-*co*-1-octene) with (a) 8.61, (b) 9.16, and (c) 11.83% molar ratios of 1-octene obtained by the Ni{$CH_3C(O)CHC[N(naphthyl)]CH_3\}_2/B(C_6F_5)_3$ system.

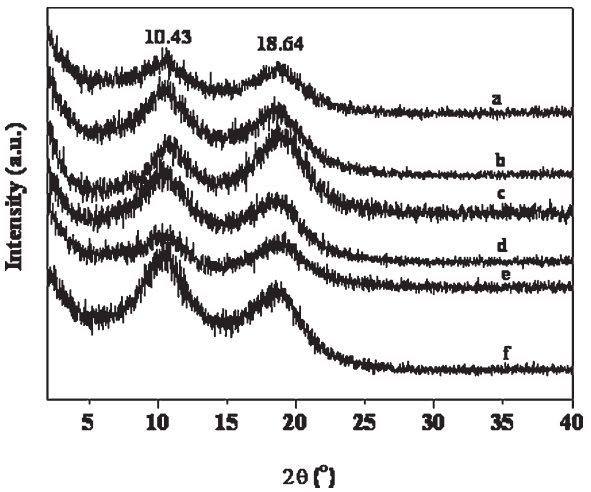

Figure 9 WAXD curves of poly(norbornene-*co*-1-hexene) with (a) 8.64, (b) 10.36, and (c) 12.85% molar ratios of 1-hexene obtained by the Ni{$CH_3C(O)CHC[N(naphthyl)]CH_3\}_2/B(C_6F_5)_3$ system; poly(norbornene-*co*-1-octene) with (d) a 9.16% molar ratios of 1-octene molar ratio obtained by the Ni{$CH_3C(O)CHC[N(naphthyl)]CH_3\}_2/B(C_6F_5)_3$ system; and poly(norbornene-*co*-1-decene) with (e) 7.88 and (f) 9.07% molar ratios of 1-decene obtained by the Ni{$CF_3C(O)CHC[N(naphthyl)]CH_3\}_2/B(C_6F_5)_3$ system.

References

1. Janiak, C.; Lassahn, P. G. J Mol Catal A 2001, 166, 193.
2. Janiak, C.; Lassahn, P. G. Macromol Rapid Commun 2001, 22, 479.
3. Kennedy, J. P.; Makowski, H. S. J Macromol Sci Chem 1967, 1, 345.
4. Gaylord, N. G.; Deshpande, A. B. J Polym Sci Polym Lett Ed 1976, 14, 613.
5. Maezawa, H.; Matsumoto, J.; Ajura, H.; Asahi, S. (to Idemitsu Kosan). Eur. Pat. 445,755 (1991); Chem Abstr 1991, 115, 256943g.
6. Goodall, B. L.; Benedikt, G. M.; Mclntosh, L. H., III; Barnes, D. A.; Rhodes, L. F. (to B. F. Goodrich Co.). U.S. Pat. 5,468,819 (1995); Chem Abstr 1995, 125, 329750k.

7. Goodall, B. L.; Risse, W.; Mathew, J. P. (to B. F. Goodrich Co.). U.S. Pat. 5,705,503 (1996); Chem Abstr 1996, 126, 104553u.
8. Barnes, D. A.; Benedikt, G. M.; Goodall, B. L.; Huang, S. S.; Kalamarides, H. A.; Lenhard, S.; Mclntosh, L. H., III; Selvy, K. T.; Shick, R. A.; Rhodes, L. F. Macromolecules 2003, 36, 2623.
9. Nishizawa, O.; Misaka, H.; Sakai, R.; Kakuchi, T.; Satoh, T. J Polym Sci Part A: Polym Chem 2008, 46, 7411.
10. Skupov, K. M.; Marella, P. R.; Hobbs, J. L.; McIntosh, L. H.; Goodall, B. L.; Claverie, J. P. Macromolecules 2006, 39, 4279.
11. Cai, Z. G.; Nakayama, Y.; Shiono, T. Macromolecules 2006, 39, 2031.
12. Boggioni, L.; Zatnpa, C.; Ravasio, A. Macromolecules 2008, 41, 5107.
13. Kaita, S.; Matsushita, K.; Tobita, M.; Maruyama, Y.; Wakatsuki, Y. Macromol Rapid Commun 2006, 27, 1752.
14. Yamashita, M.; Takamiya, I.; Jin, K.; Nozaki, K. Organometallics 2006, 25, 4588.
15. Takamiya, I.; Yamashita, M.; Murotani, E.; Morizawa, Y.; Nozaki, K. J Polym Sci Part A: Polym Chem 2008, 46, 5133.
16. Huang, C. F.; Wang, S. K.; Kuo, S. W.; Huang, W. J.; Chang, F. C. J Appl Polym Sci 2004, 92, 1824.
17. Jung, H. Y.; Hong, S.-D.; Jung, M. W.; Lee, H.; Park, Y.-W. Polyhedron 2005, 24, 1269.
18. Kaminsky, W.; Hoff, M.; Derlin, S. Macromol Chem Phys 2007, 208, 1341.
19. Li, X.; Nishiura, M.; Mori, K.; Mashiko, T.; Hou, Z. Chem Commun 2007, 40, 4137.
20. Shiono, T.; Sugimoto, M.; Hasan, T.; Cai, Z. G.; Ikeda, T. Macromolecules 2008, 41, 8292.
21. He, X. H.; Yao, Y. Z.; Luo, X.; Zhang, J. K.; Liu, Y. H.; Zhang, L.; Wu, Q. Organometallics 2003, 22, 4952.
22. He, X. H.; Wu, Q. Appl Organomet Chem 2006, 20, 264.
23. Zhu, Y. Z.; Liu, J. Y.; Li, Y. S.; Tong, Y. J. J Organomet Chem 2004, 689, 1295.
24. Kelen, T.; Tüdõs, F. J Macromol Sci Pure Appl Chem 1975, 9, 1.
25. Leone, G.; Boglia, A.; Boccia, A. C.; Scafati, S. T.; Bertini, F.; Ricci, G. Macromolecules 2009, 42, 9231.
26. Gao, H. Y.; Chen, Y.; Zhu, F. M.; Wu, Q. J Polym Sci Part A: Polym Chem 2006, 44, 5237.
27. Benedikt, G. M.; Elec, E.; Goodall, B. L.; Kalamarides, H. A.; Mclntosh, L. H., III; Selvy, K. T.; Rhodes, L. F.; Selvy, K. T. Macromolecules 2002, 35, 8978.
28. Sacchi, M. C.; Sonzogni, M.; Losio, S.; Forlin, F.; Locatelli, P.; Tritto, I.; Licchelli, M. Macromol Chem Phys 2001, 202, 2052.
29. Wilks, B. R.; Chung, W. J.; Ludovice, P. J.; Rezac, M. R.; Meakin, P.; Hill, A. J. J Polym Sci Part B: Polym Phys 2003, 41, 2185.
30. He, F. P.; Chen, Y. W.; He, X. H.; Chen, M. Q.; Zhou, W. H.; Wu, Q. J Polym Sci Part A: Polym Chem 2009, 47, 3990.